Preliminary report of liquefaction phenomena triggered by the March 2021 earthquakes in Central Thessaly, Greece

S. Valkaniotis, G. Papathanassiou, Ath. Ganas, E. Kremastas, R. Caputo

Preliminary report of liquefaction phenomena triggered by the March 2021 earthquakes in Central Thessaly, Greece

Valkaniotis S.[1], Papathanassiou G.[1], Ganas Ath.[2], Kremastas E.[3], Caputo R.[4]

1 Department of Civil Engineering, Democritus University of Thrace, Greece
valkaniotis@yahoo.com, gpapatha@civil.duth.gr
2 Geodynamic Institute, National Observatory of Athens, Greece
aganas@noa.gr
3 Department of Geology, Aristotle University of Thessaloniki, Greece
ekremast@geo.auth.gr
4 Department of Physics and Earth Sciences, University of Ferrara, Italy
rcaputo@unife.it

DOI: 10.5281/zenodo.4608365

The report is available in the Zenodo repository: https://doi.org/10.5281/zenodo.4608365

March 16, 2021

On the 3rd and 4th of March 2021, two strong earthquakes of M6.3 and M6.0, respectively occurred at Thessaly, Central Greece. Distribution of aftershocks and events of M>5 for the sequence are shown in Figure 1. This sequence is considered as the most hazardous one regarding the triggering of liquefaction phenomena in Greece the last 40 years. Liquefaction is the transformation of saturated, unconsolidated granular material from a solid state to a liquid state as a consequence of increased pore pressures that reduce the effective strength of the material (Youd, 1973). The loss of shear strength can cause permanent ground deformations and damage to man-made structures.

During extensive field survey and mapping, accompanied by UAV aerial surveys, following the strong earthquakes, numerous (more than 400 cases) liquefaction-related features were identified, including sand blows and craters, fissures and lateral spreading cracks/ruptures along the Pinios and Titarisios river banks. A rapid documentation of these features was important, as most of these features were going to be erased or smoothed by the ploughing season that is ongoing in the area.

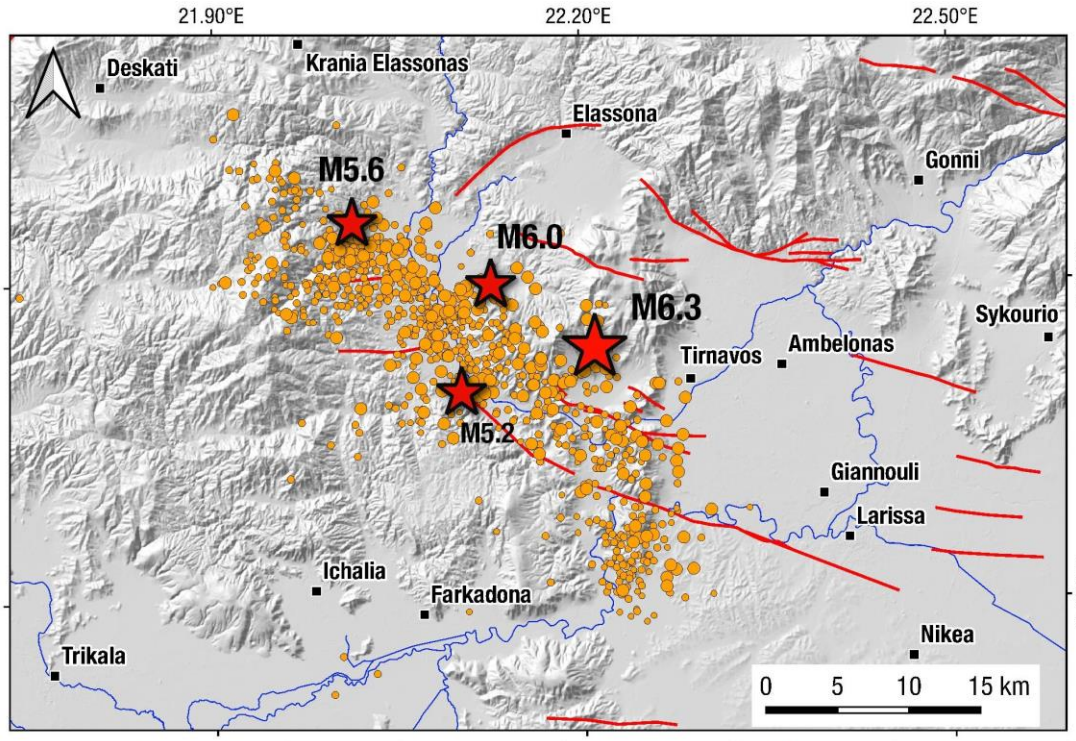

Date	Time	Latitude	Longitude	Magnitude	Depth (km)
March 3, 2021	10:16:08	39.7591	22.2102	6.3	8.5
March 3, 2021	11:45:46	39.6996	22.2478	5.1	7.1
March 3, 2021	18:24:08	39.7316	22.1013	5.2	6.4
March 4, 2021	18:38:19	39.7993	22.126	6.0	4.8
March 4, 2021	19:23:51	39.8373	21.9424	5.1	9.4
March 12, 2021	12:57:51	39.8387	22.0134	5.6	7.0

Figure 1. Location map with epicenters (orange) of the March 2021 Thessaly, Greece earthquake. Epicenter data from the revised NOA catalogue. Events with magnitude larger than 5 are shown as red stars. Active faults, from the NOAFaults database and modified from Caputo (1995), with red lines.

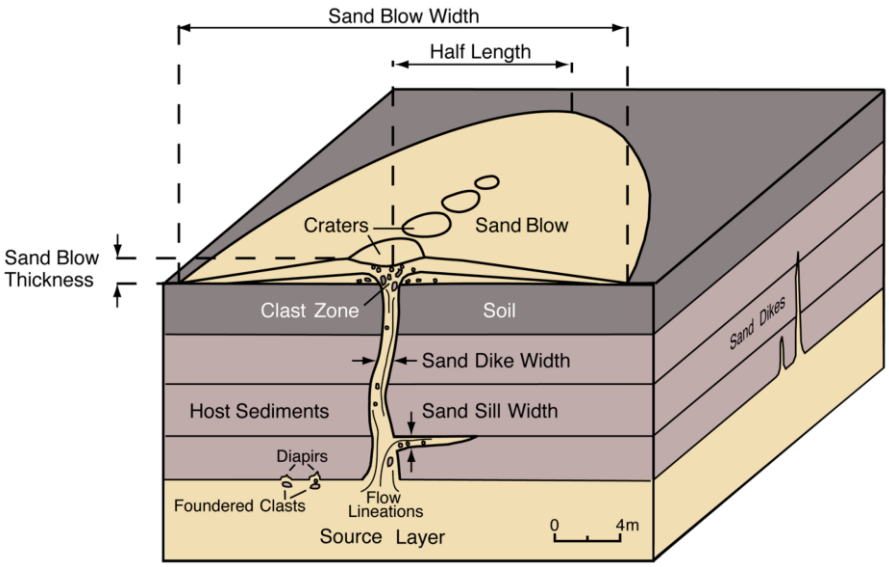

Figure 2. Schematic diagram showing liquefied layers and overlying liquefaction features, including intrusive sand dikes and sills and an extrusive sand blow. From Tuttle (2019).

Interferograms created using Copernicus Sentinel-1 radar imagery reveal the extent of areas with liquefaction and lateral spreading phenomena. In Figure 3, coherence from the coseismic interferogram and a pre-event interferogram are compared, highlighting two large areas of low coherence along Titarisios river to the north (Figure 4) and Pinios river to the south. Low coherence in interferograms corresponds to either spots with low correlation (due to presence of water, change of land use etc) or areas with ground displacement characterized by high frequency lateral heterogeneities and/or surface disturbance.

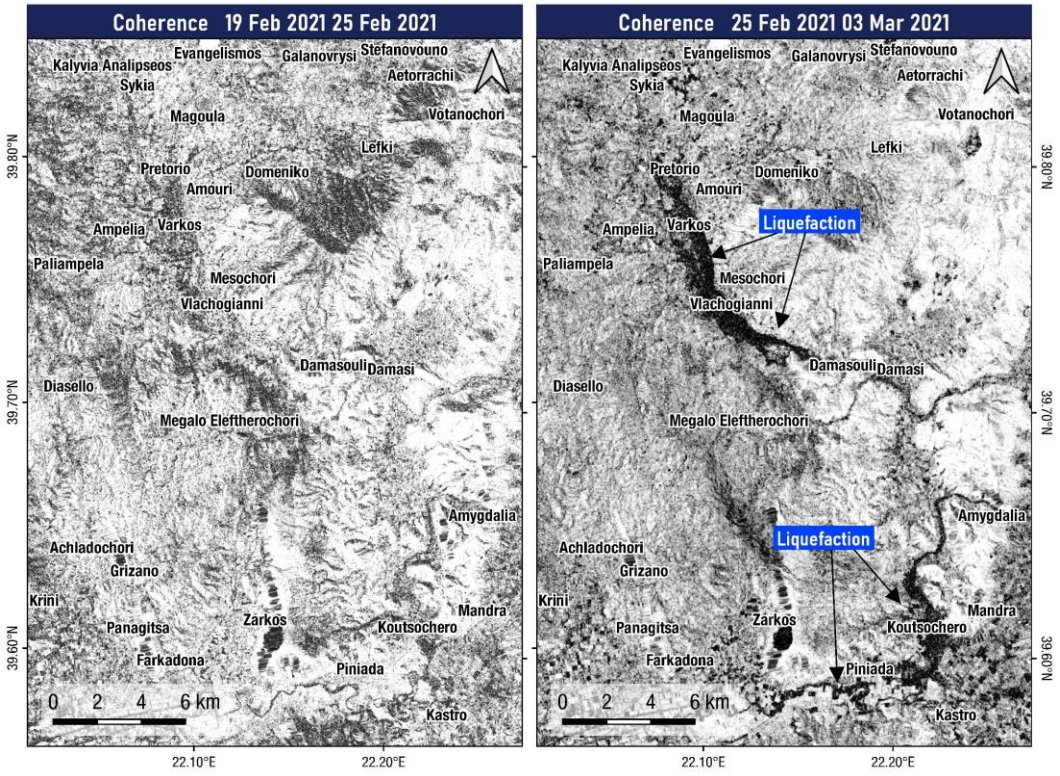

Figure 3. Difference of coherence in interferograms pre-event(left) and coseismic (right). Dark areas of low coherence correspond to areas of widespread liquefaction and lateral spreading.

As those two low coherence areas do not appear in interferograms before and after the earthquake, we consider those as areas of widespread liquefaction and lateral spreading. This was also validated by the field survey.

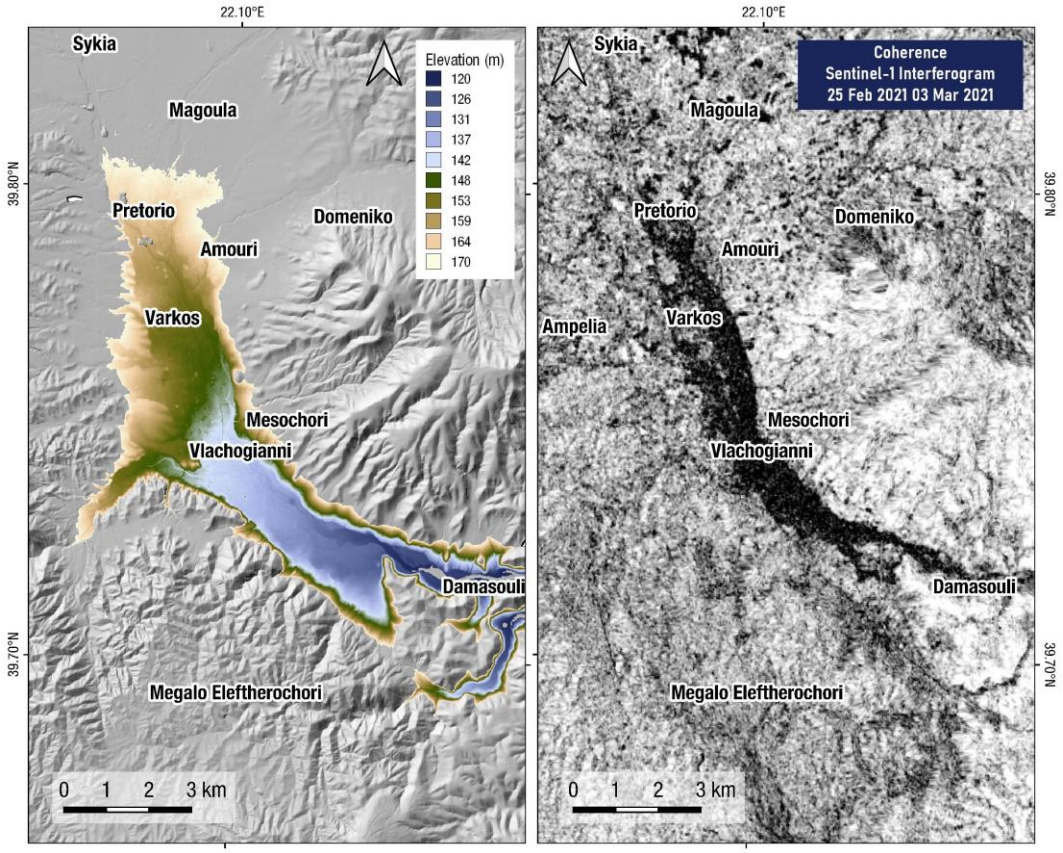

Figure 4. Left: elevation map of Titarisios river valley between Pretorio and Damasouli (only elevations between 120 and 170 m.a.s.l. are shown). Right: Low coherence in the coseismic Sentinel-1 interferogram correspond to liquefaction along Titarisios river bed and floodplain.

The maximum length of the ground fissures generated by liquefaction, from where a mixture of sandy and silty material was ejected, was 60m while the maximum diameter and depth of sand craters was 2.5m and 1.5m, respectively. The majority of the liquefaction surface manifestations were reported on a zone of approximately 10km length and 1km width around Pinios river and between the settlements of Farkadona, Zarko and Koutsochero, along the so called Piniada valley (Caputo et al 2021). A large number (but less concentrated) of liquefaction features were additionally documented between the villages Varko and Damasi along Titarisios river floodplain, situated at the epicentral area of both earthquakes.

The former area is geomorphologically characterized as a flood plain that periodically covered by the flooding material of Pinios river (Figures 5 & 6, Mantovani et al. 2018, Caputo et al. 2021) and it had been classified as highly susceptible to liquefaction by Papathanassiou et al. (2010). In addition, within this liquefiable zone, the Pinios river formed many meanders that are classified as one of the most prone to liquefaction areas; particularly the areas of point bar deposits that developed in the inside bank of Pinios river meanders.

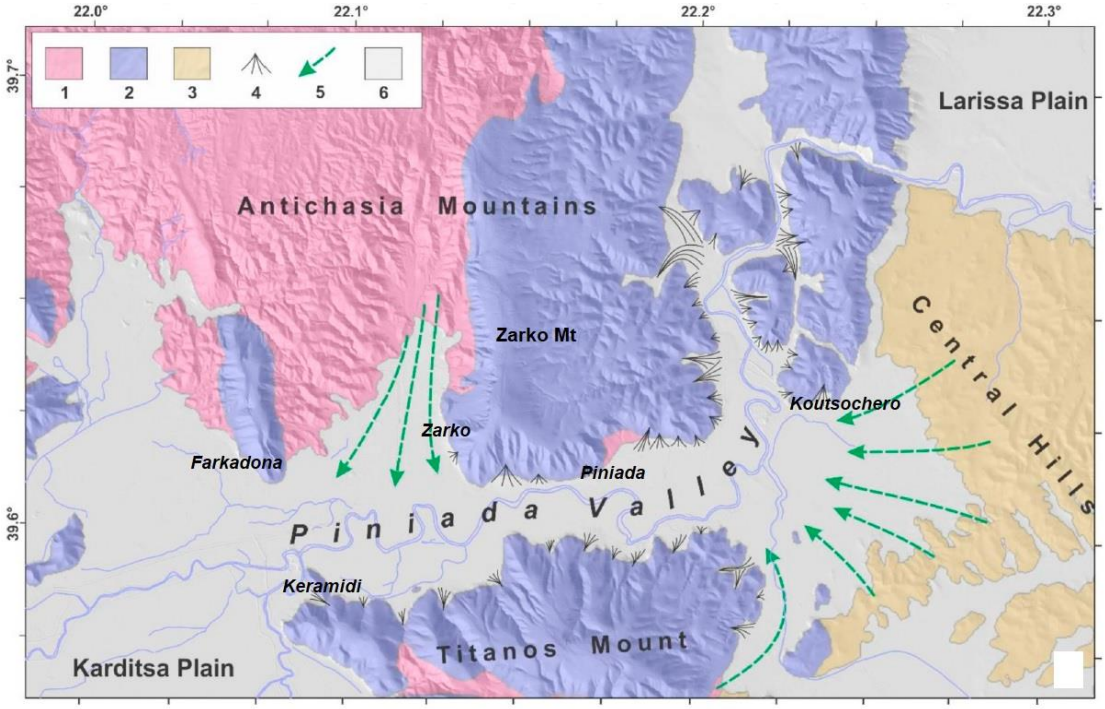

Figure 5. Simplified geologic map of Pinios river study area (from Caputo et al. 2021). 1: Palaeozoic gneiss and schists; 2: Triassic-Lower Jurassic recrystallized limestones; 3: Pliocene-Early Pleistocene fluvio-lacustrine deposits; 4: Late Pleistocene alluvial cones (from carbonate rocks); 5: Late Pleistocene alluvial cones (from Palaeozoic and Neogene-Quaternary rocks): 6: Late Quaternary alluvial deposits.

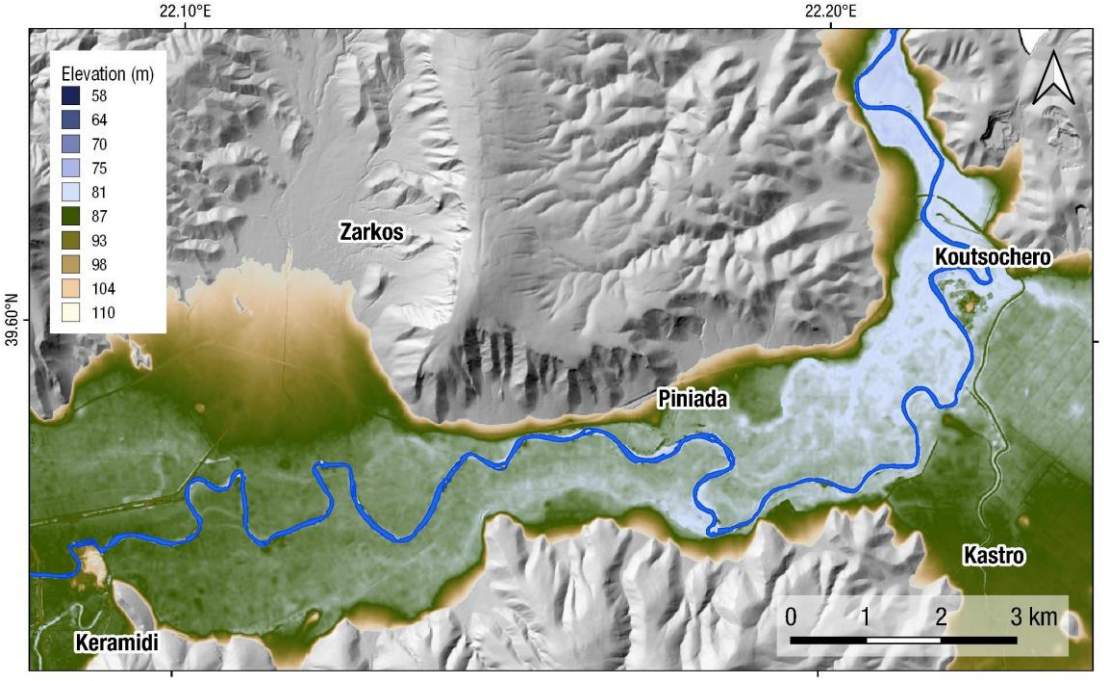

Figure 6. Elevation map of the Pinios river valley strand between Zarko and Koutsochero (only elevations between 58 and 120 m.a.s.l. are shown). A 1-2 km wide valley can be seen to form along the meandering river bed of Pinios river.

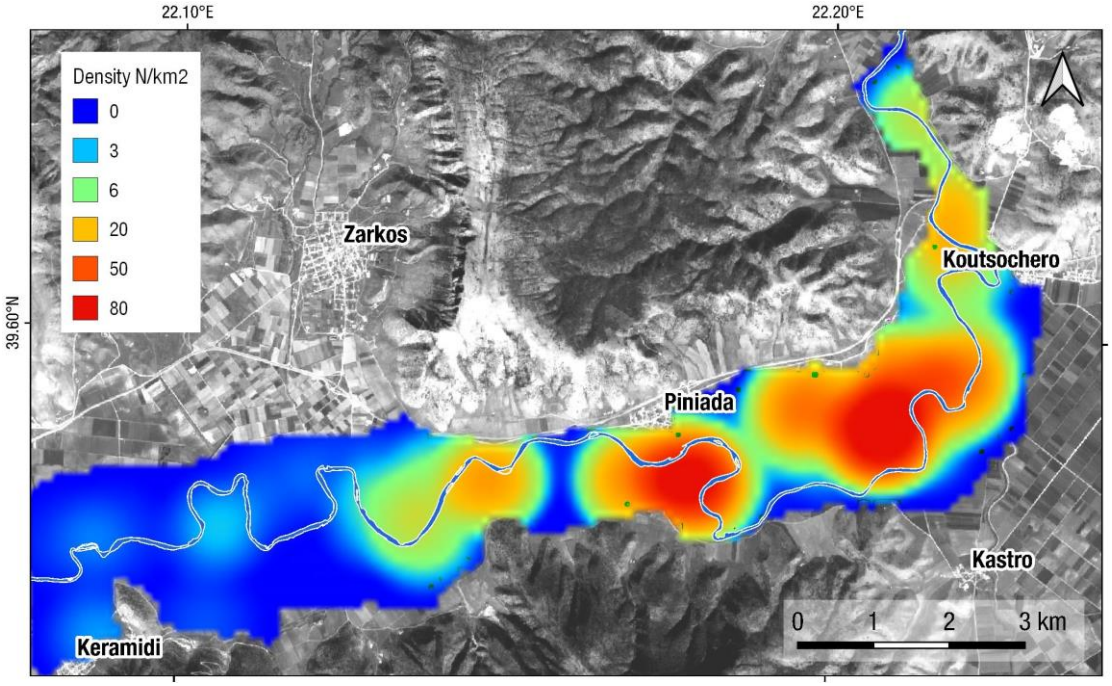

Figure 7. Density (number per square kilometer) of mapped liquefaction features along Pinios river.

As it is shown in the compiled relevant map (Figure 7), the spatial distribution of the liquefied sites is strongly related not only to the present locations of meanders but mainly to oxbow lake areas that formed as the remains of the bend in the river. In order to spatially correlate the locations of the liquefied sites with the oxbow lakes, we took into account historical aerial imagery (Hellenic Army Geographical Service) and multi-temporal optical satellite imagery. As a preliminary result of our research, we concluded that the highest density values of liquefaction phenomena are concentrated within the point bar areas of these abandoned meanders. In Figure 8, it is shown an example of the spatial distribution of the liquefaction-induced phenomena in the inside bank of an oxbow lake, as it can be clearly delineated based on the aerial imagery of 1945.

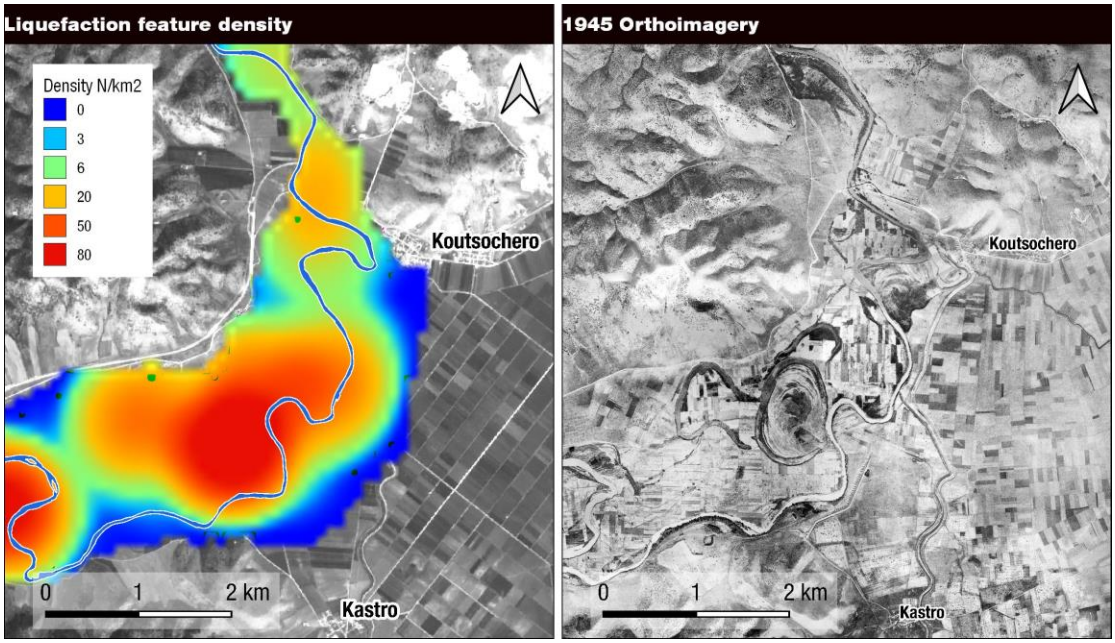

Figure 8. Left: density map of liquefaction features (number per square kilometer). Right: 1945 orthoimagery (from Hellenic Army Geographical Service).

References

Caputo R. 1995. Inference of a seismic gap from geological data: Thessaly (Central Greece) as a case study. Ann. Geofisica, 38 (1), 1-19 https://doi.org/10.4401/ag-4127

Caputo R., Helly B., Rapti D., Valkaniotis S. 2021. Late Quaternary hydrographic evolution in Thessaly (Central Greece): The crucial role of the Piniada Valley. Quaternary International, https://doi.org/10.1016/j.quaint.2021.02.013

Mantovani A., Valkaniotis S., Rapti D., Caputo R. 2018. Mapping the palaeo-Piniada Valley, Central Greece, based on systematic microtremor analyses. Pure Appl. Geophys. 175, 865–881. https://doi.org/10.1007/s00024-017-1731-7

Papathanassiou G., Valkaniotis S., Chaztipetros Al., Pavlides S. 2010. Liquefaction susceptibility map of Greece, Proc. Of the 12th International Conference of Greek Geological Society, Bulletin of the Geological Society of Greece, vol. XLIII, No3, 1383-1392

Tuttle M.P., Hartleb R. Wolf, L. Mayne, P.W. 2019. Paleoliquefaction Studies and the Evaluation of Seismic Hazard. *Geosciences*, *9*, 311. https://doi.org/10.3390/geosciences9070311

Youd T.L. 1973. Liquefaction, flow and associated ground failure: U.S. Geological Survey Circular 688,12 pp.

Figure 9. Liquefaction fissure with ejected sand (Photo taken by G. Papathanassiou 07/03/2021).

Figure 10. Sand crater (Photo taken by G. Papathanassiou 05/03/2021).

Figure 11. Aerial view of multiple linear liquefaction fissures (Photo taken by G. Papathanassiou 05/03/2021).

Figure 12. Lateral spreading along Pinios river (Photos taken by S. Valkaniotis 05/03/2021).

Figure 13. Liquefaction fissure with ejected sand (Photo taken by A. Ganas 06/03/2021).

Figure 14. Liquefaction fissure with ejected sand (Photo taken by S. Valkaniotis 05/03/2021).

Figure 15. Close-up of liquefaction fissure with small craters (Photo taken by S. Valkaniotis 05/03/2021).